Magnetically Alignable Phase of Phospholipid "Bicelle" Mixtures Is a Chiral Nematic Made Up of Wormlike Micelles

Mu-Ping Nieh,[†,‡] V. A. Raghunathan,[‡,§] Charles J. Glinka,[∥] Thad A. Harroun,[‡] Georg Pabst,[⊥] and John Katsaras*[,‡]

Department of Physics, University of Guelph, Guelph, Ontario, N1G 2W1, Canada, National Research Council, Steacie Institute for Molecular Sciences, Chalk River, Ontario, K0J 1J0, Canada, Raman Research Institute, Bangalore 560 080, India, National Institute of Standards and Technology, Gaithersburg, Maryland 20899, and Institute of Biophysics and X-ray Structure Research, Austrian Academy of Sciences, Schmiedlstrasse 6, A-8042 Graz, Austria

Received June 2, 2004. In Final Form: July 28, 2004

We have studied the phase behavior of binary mixtures of long- and short-chain lipids, namely, dimyristoyl phosphatidylcholine (DMPC) and dihexanoyl phosphatidylcholine (DHPC), using optical microscopy and small-angle neutron scattering. Samples with a total lipid content of 25 wt %, corresponding to ratios Q ([DMPC]/[DHPC]) of 5, 3.2, and 2, are found to exhibit an isotropic (I) → chiral nematic (N*) → lamellar phase sequence on increasing temperature. The I−N* transition coincides with the chain melting transition of DMPC at $Q = 5$ and 3.2, but the N* phase forms at a higher temperature for $Q = 2$. All three samples form multilamellar vesicles in the lamellar phase. Our results show that disklike "bicellar" aggregates occur only in the lower temperature isotropic phase and not in the higher temperature magnetically alignable N* phase, where they were previously believed to exist. The N* phase is found to consist of long, flexible wormlike micelles, their entanglement resulting in the very high viscosity of this phase.

1. Introduction

Amphiphilic molecules self-assemble in water to form a variety of aggregates whose morphology is governed by the relative size of their hydrophilic and hydrophobic moieties.[1] Phospholipids with two long hydrocarbon chains, such as dimyristoyl phosphatidylcholine (DMPC), form bilayers over a wide range of temperature and water content. On the other hand, lipids with short chains, such as dihexanoyl phosphatidylcholine (DHPC), generally form micelles. Binary mixtures of long- and short-chain lipids, therefore, tend to form aggregates that can accommodate these conflicting geometric constraints imposed by the two components. For example, DMPC−DHPC mixtures are known to form disklike micelles, often called bicelles, with DHPC molecules preferentially occupying the rim of the disk.[2] At higher temperatures, bilayers riddled with porelike defects are formed, with the DHPC molecules found lining their edges.[3] The partial segregation of the two lipid species within bicelles and bilayers creates microenvironments that are analogous to those found in aggregates formed by DMPC or DHPC individually. Similar behavior has also been observed in mixtures of lipids with detergents and in some binary mixtures of cationic and anionic surfactants.[4−6]

DMPC−DHPC mixtures are used in high-resolution NMR experiments to align membrane proteins as well as water-soluble macromolecules.[7−12] Despite their widespread use, only a few investigations of their thermodynamic phase behavior have so far been reported.[3,13−17] Partial phase diagrams of these mixtures have been determined from small-angle neutron scattering (SANS) data, with and without a charged dopant, such as dimyristoyl phosphatidylglycerol (DMPG) or Tm^{3+}.[3,17] The phase behavior of these mixtures is found to be very different from those of the individual lipids, due mainly to the different morphology of the mixed aggregates.

For NMR applications, the most relevant phase formed by these lipid mixtures is the one that occurs at intermediate temperatures, typically around 30 °C. This magnetically alignable phase has not been fully characterized, although it has often been described in the literature as a nematic phase consisting of bicelles. However, this morphology does not account for the very high viscosity of this phase. There has also been some

* Corresponding author. E-mail: john.katsaras@nrc.gc.ca. Fax: 613-584-4040. Phone: 613-584-8811, extension 3984.
† Department of Physics, University of Guelph.
‡ National Research Council, Steacie Institute for Molecular Sciences.
§ Raman Research Institute.
∥ National Institute of Standards and Technology.
⊥ Institute of Biophysics and X-ray Structure Research, Austrian Academy of Sciences.

(1) Israelachvili, J. *Intermolecular and Surface Forces*, 2nd ed.; Academic Press: Oxford, 2000.
(2) Sanders, C. R., II; Schwonek, J. *Biochemistry* **1992**, *31*, 8898.
(3) Nieh, M.-P.; Glinka, C. J.; Krueger, S.; Prosser, R. S.; Katsaras, J. *Langmuir* **2001**, *17*, 2629.
(4) Lang, J.; Egelhaaf, S. U.; Cates, M. E. *Biophys. J.* **2003**, *85*, 1624.
(5) Funari, S.; Nuscher, B.; Rapp, G.; Beyer, K. *Proc. Natl. Acad. Sci. U.S.A.* **2001**, *98*, 8938.
(6) Zemb, Th.; Dubois, M.; Demè, B.; Gulik-Krzywicki, Th. *Science* **1999**, *283*, 816.
(7) Vold, R. R.; Prosser, R. S.; Deese, A. J. *J. Biomol. NMR* **1997**, *9*, 329.
(8) Tjandra, N.; Bax, A. *Science* **1997**, *278*, 1111.
(9) Sanders, C. R.; Prosser, R. S. *Structure* **1998**, *6*, 1227.
(10) Prosser, R. S.; Volkov, V. B.; Shiyanovskaya, I. V. *Biochem. Cell Biol.* **1998**, *76*, 443.
(11) Sternin, E.; Nizza, D.; Gawrisch, K. *Langmuir* **2001**, *17*, 2610.
(12) Bax, A. *Protein Sci.* **2003**, *12*, 1.
(13) Katsaras, J.; Donaberger, R. L.; Swainson, I. P.; Tennant, D. C.; Tun, Z.; Vold, R. R.; Prosser, R. S. *Phys. Rev. Lett.* **1997**, *78*, 899.
(14) Raffard, G.; Steinbrucker, S.; Arnold, A.; Davis, J. H.; Dufourc, E. J. *Langmuir* **2000**, *16*, 7655.
(15) Gaemers, S.; Bax, A. *J. Am. Chem. Soc.* **2001**, *123*, 12343.
(16) Luchette, P. A.; Vetman, T. N.; Prosser, R. S.; Hancock, R. E. W.; Nieh, M.-P.; Glinka, C. J.; Krueger, S.; Katsaras, J. *Biochim. Biophys. Acta* **2001**, *1513*, 83.
(17) Nieh, M.-P.; Glinka, C. J.; Krueger, S.; Prosser, R. S.; Katsaras, J. *Biophys. J.* **2002**, *82*, 2487.

10.1021/la048641l CCC: $27.50
Published on Web 08/19/2004

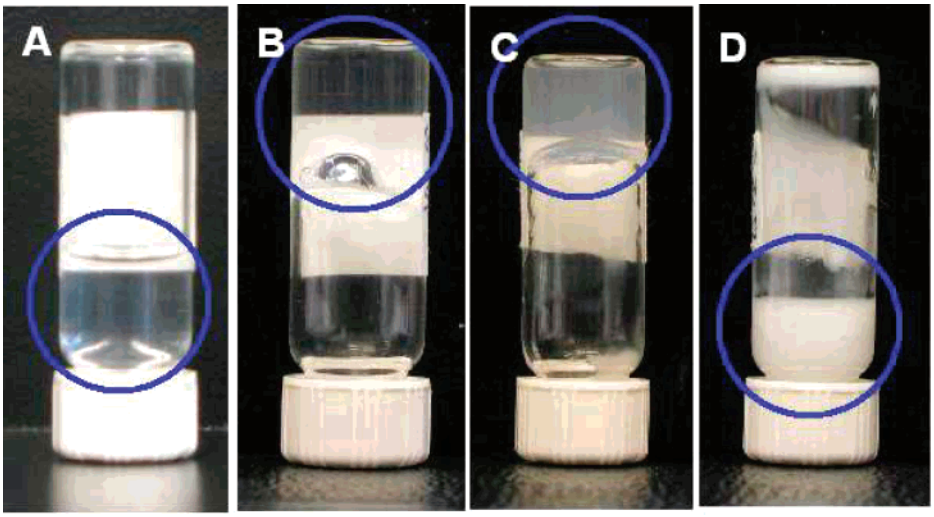

Figure 1. The $Q = 2$ sample is transparent for $T < 20$ °C and has a viscosity comparable to that of water (A). However, for 30 °C $< T <$ 40 °C the sample becomes highly viscous (B). The $Q = 5$ sample is slightly turbid and highly viscous for 23 °C $< T <$ 30 °C (C). It turns opaque above 30 °C with a concomitant decrease in viscosity (D). The labels on the bottles appear as white strips, while the circles indicate the location of the sample in the bottles.

speculation that this phase is made up of an interconnected network of lipid aggregates.[9] On the other hand, it is now well established that the addition of a charged dopant transforms this phase into a lamellar phase, consisting of bilayers populated with porelike defects that are stabilized by the short-chain lipid molecules.[3,13]

Here we present a detailed characterization of the phase behavior of aqueous solutions of DMPC−DHPC mixtures, using a combination of scattering and optical microscopy techniques. Three samples corresponding to a [DMPC]/[DHPC] molar ratio, Q, of 5, 3.2, and 2 and a total lipid concentration (DMPC + DHPC) of 25 wt % were studied. In agreement with earlier reports, we find an isotropic bicellar solution in all the samples below the chain melting transition temperature (T_M) of DMPC. At higher temperatures, a chiral nematic phase is found, which transforms, with increasing temperature, into a dispersion of multilamellar vesicles (MLV). The present study clearly shows that the magnetically alignable phase of these systems is not comprised of the disklike bicelles, as had been proposed earlier, but instead consists of wormlike micelles, very similar to the ones found in some surfactant solutions.[18]

2. Experimental Section

DMPC and DHPC were purchased from Avanti Polar Lipids (Alabaster, AL) and were used without further purification.[19] They were dissolved in D_2O (99.9% purity, Chalk River Laboratories) at a total lipid concentration of 25 wt %. Three samples were prepared with molar ratio, Q ([DMPC]/[DHPC]), equal to 5, 3.2, and 2.

For polarized optical microscopy (POM) observations, samples were taken in sealed rectangular glass capillaries (2 mm × 0.1 mm, VitroCom Inc., Mountain Lakes, NJ). The Olympus BX52 microscope was equipped with a 3 megapixel CCD camera and a Linkam THMS600 temperature-controlled stage (Surrey, U.K.) with an accuracy of ±0.05 °C. Each sample was equilibrated at the desired temperature for at least 30 min prior to experimentation.

SANS experiments were performed on the 30-m SANS instrument (NG7) at the National Institute of Standards and Technology (Gaithersburg, MD). Two sample-to-detector distances (1.25 and 15.3 m) were used to cover a range of the magnitude of scattering vectors, q ($=4\pi \sin(\theta/2)/\lambda$, where θ and λ are the scattering angle and the neutron wavelength, respectively), from 0.002 to 0.35 Å^{-1}. Samples for SANS studies were loaded in quartz cells with a path length of 2 mm and were placed in a block, whose temperature was controlled using a circulating water bath. Each measurement was taken after the sample was equilibrated at the desired temperature for ∼30 min. Data collected on a two-dimensional detector were corrected for background and reduced to the absolute scale. They were then circularly averaged to get the scattered intensity as a function of q.

3. Results and Discussion

The appearance and viscosity of the samples change considerably with temperature, T. For T below ∼25 °C, all of the samples are clear with viscosities comparable to that of water (Figure 1A). However, they become very viscous and gel-like at around 25 °C. Even at 25 °C, the $Q = 2$ and 3.2 samples remain quite clear (Figure 1B); however, the same cannot be said of the $Q = 5$ sample, which becomes translucent in appearance (Figure 1C). As T is further increased, the viscosity of all the samples drops significantly, and concomitantly they all turn opaque (Figure 1D). The temperature at which this happens varies with Q, being around 30, 55, and 65 °C for $Q = 5$, 3.2, and 2 samples, respectively. This nonmonotonic T dependence of viscosity is consistent with earlier reports of DMPC−DHPC mixtures.[20,21]

On increasing T, POM observations indicate the occurrence of two phase transitions in all three samples. At low temperatures, an isotropic (I) phase is observed which transforms into a chiral nematic (N*) phase at higher T and gives rise to a fingerprint texture (Figure 2). The nematic (N) phase is characterized by long-range orientational ordering of anisotropic (usually rodlike or disklike) aggregates, with short-range positional order as in an isotropic liquid. The preferred direction of orientation is described by a unit vector $\hat{n}$, called the director. In the presence of chiral molecules, this phase develops a spontaneous twist deformation about an axis normal to $\hat{n}$, forming the N* phase.[22] The pitch of this twisted

(18) Candau, S. J.; Lequeux, F. *Curr. Opin. Colloid Interface Sci.* **1997**, *2*, 420.
(19) The identification of any commercial product or trade name does not imply endorsement or recommendation by the National Institute of Standards and Technology.
(20) Hwang, J. S.; Oweimreen, G. A. *Arab J. Sci. Eng.* **2003**, *28*, 43.
(21) Struppe, J.; Vold, R. R. *J. Magn. Reson.* **1998**, *135*, 541.
(22) de Gennes, P. G.; Prost, J. *The Physics of Liquid Crystals*, 2nd ed.; Clarendon Press: Oxford, 1993.

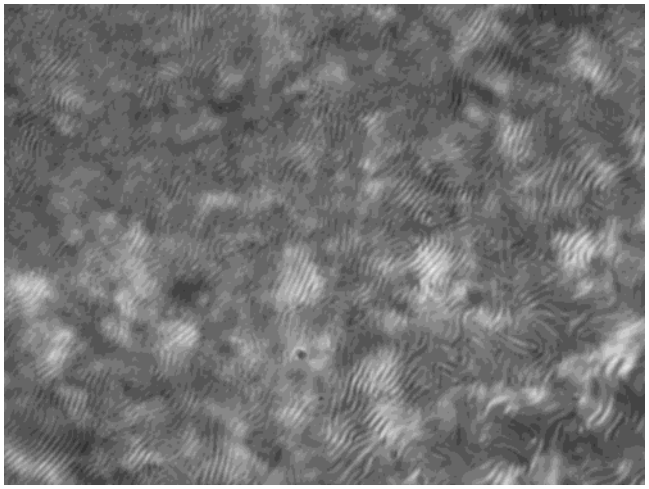

Figure 2. Polarized optical microscopy image of the $Q = 5$ sample at 23.5 °C, showing the fingerprint texture characteristic of the chiral nematic (N*) phase.

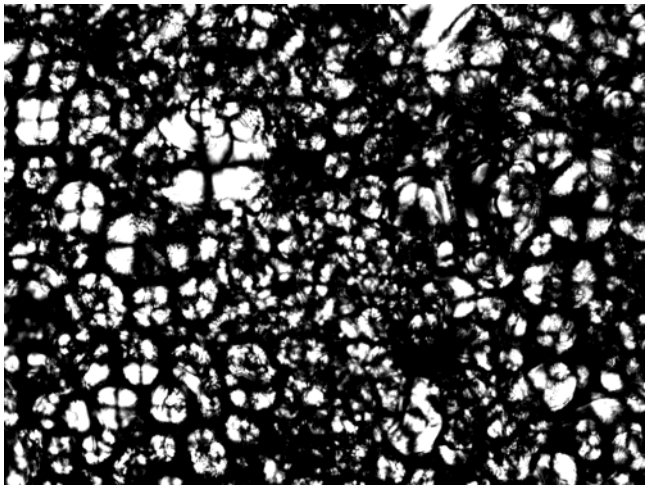

Figure 3. Polarized optical microscopy image of the $Q = 5$ sample at 30 °C, which shows the "Maltese cross" texture characteristic of a dispersion of multilamellar vesicles in an isotropic solution.

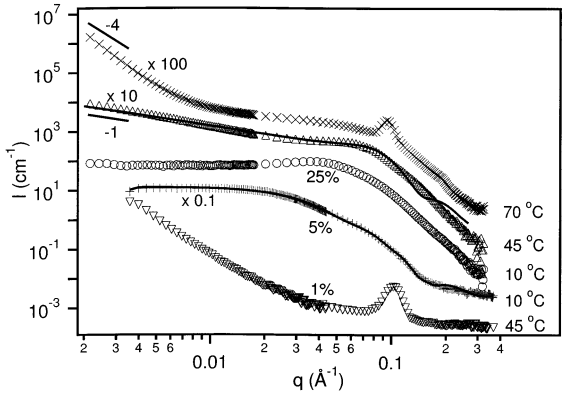

Figure 4. SANS data of the 25 wt %, $Q = 3.2$ sample in the isotropic (10 °C), nematic (45 °C), and lamellar (70 °C) phases. The curves have been shifted vertically for clarity by the factors indicated. Data from a 5 wt % sample in the isotropic phase at 10 °C and a 1 wt % sample in the lamellar phase at 45 °C are also shown for comparison. The solid curves are fits to models whose details are given in the text. Note that the lamellar phase appears at lower temperatures in the dilute sample.

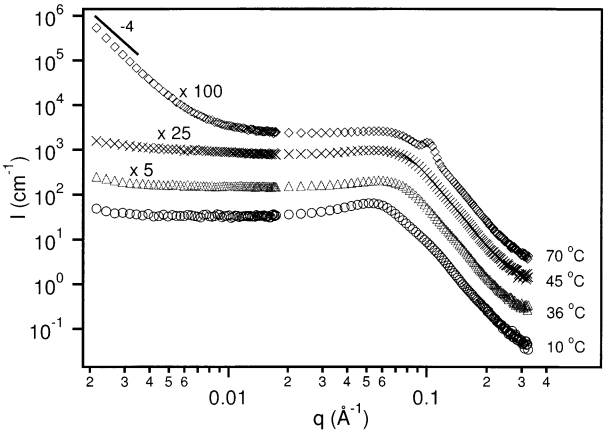

Figure 5. SANS data of the $Q = 2$, 25 wt % sample in the low- and high-viscosity isotropic phases (10 and 36 °C, respectively), in the I−N* two-phase region (45 °C), and in the MLV dispersion (70 °C). For clarity, the curves have been shifted vertically by the multiplicative factors indicated.

structure is generally in the 0.1−10 μm range and leads to the fingerprint texture seen under the microscope (Figure 2). The isotropic → N* transition temperature, T_{IN^*}, takes place at ∼23 °C for $Q = 5$ and 3.2 samples. On the other hand, the isotropic phase is stable up to 41 °C in the $Q = 2$ sample, above which an I−N* coexistence phase begins. A pure N* phase is not found in this sample. On increasing the temperature further, all three samples show a Maltese cross texture, typical of MLV in an isotropic solution (Figure 3). The temperature at which this transition occurs also depends on Q and is ∼27, 53, and 65 °C for $Q = 5$, 3.2, and 2 samples, respectively.

SANS data were collected from the three samples at different temperatures. Data from the three phases of the $Q = 5$ and 3.2 samples are very similar; hence only the latter are shown in Figure 4. For comparison, in the same figure we also present the scattering pattern of a 5 wt % solution at 10 °C. The scattering pattern of the 25 wt % solution at the same T shows a broad peak at $q = 0.04$ Å^{-1}, which is absent in the more dilute case. The pattern of the N* phase at 45 °C also shows a broad peak, but the most pertinent feature is the significant increase in the scattered intensity at low q values. This feature becomes even more prominent at higher temperatures, when the sample transforms into a dispersion of MLV. At these temperatures, the scattering pattern also contains a sharp peak ($q \sim 0.1$ Å^{-1}) due to the regular stacking of the bilayers making up the MLV. The lamellar repeat spacing, d, at 70 °C is 66 Å, similar to the d of pure liquid crystalline DMPC bilayers.[23,24] The scattering curves of the $Q = 2$ sample (Figure 5) show a much less pronounced dependence on temperature in the isotropic phase and in the I−N* coexistence region, with a slight increase in the scattering at small q with increasing T. However, at 70 °C, the scattered intensity at small q increases significantly due to the presence of MLV, as was the case in the other two samples.

The SANS profile of the dilute solution at 10 °C (Figure 4) can be fitted to the form factor of a bicelle of radius 80 Å and thickness 50 Å.[3] We believe that at 10 °C 25 wt % samples are also made up of bicelles, although we have not tried to model their structure due to the complications introduced by the structure factor $S(q)$ contribution at this lipid concentration, which is likely responsible for the broad peak seen in the scattering patterns. The occurrence of bicelles in the isotropic phase of all the

(23) Katsaras, J. *Biophys. J.* **1998**, *75*, 2157.
(24) Pabst, G.; Katsaras, J.; Raghunathan, V. A.; Rappolt, M. *Langmuir* **2003**, *19*, 1716.

solutions for $T < 23$ °C is consistent with the observed low viscosity of these samples.

The I−N* transition of the $Q = 5$ and 3.2 samples accompanies the chain melting transition of DMPC, which occurs at ∼23 °C. The chiral nature of this phase is due to the intrinsic chirality of the lipid molecules and results in the spontaneous twisting of the nematic structure.[22] From the periodicity of the fingerprint texture, similar to Figure 2, the pitch of this helical structure can be deduced to be of the order of 10 μm. The dramatic increase in the viscosity of these two samples accompanying the I−N* transition suggests the formation of large lipid aggregates, possibly long, flexible wormlike micelles (WLM). Isotropic and nematic phases of such micelles are well-known and are usually highly viscous due to the entanglement of the long polymer-like aggregates.[18] It is possible that these aggregates are also interconnected, as in some surfactant systems.[25] In the present case, these aggregates are expected to be ribbonlike, rather than cylindrical, due to the tendency of DMPC to form bilayers. Presumably, the edges of these ribbonlike structures are preferentially occupied by the DHPC molecules. The presence of such structures is also suggested by the SANS data, which show a linear decrease of the scattered intensity over a decade of q, and characteristic of the form factor of linear aggregates (Figure 4).

To confirm this possibility, we have fitted the observed intensity to that calculated from a model (Figure 4). The scattered intensity $I(q) \propto P(q)S(q)$, where $P(q)$ is the aggregate form factor and $S(q)$ is the structure factor of the solution. The organization of the aggregates in a plane normal to the nematic director can be described, to a good approximation, by the structure factor $S_{2D}(q)$ of a two-dimensional liquid,[26,27] which to first order is described by a two-dimensional hard disk fluid[28] as follows:

$$\frac{1}{S(q_\perp)} = 1 + 4\eta\left\{A\left[\frac{J_1(q_\perp R)}{q_\perp R}\right]^2 + B\frac{J_0(q_\perp R)J_1(q_\perp R)}{q_\perp R} + G\frac{J_1(2q_\perp R)}{q_\perp R}\right\}$$

$G = 1/(1-\eta)^{3/2}$, $\chi = (1+\eta)/(1-\eta)^3$, $A = [1 + (2\eta - 1)\chi + 2\eta G]/\eta$, $B = [(1-\eta)\chi - 1 - 3\eta G]/\eta$. η is the packing fraction of the disks, R is the disk radius, and J_0 and J_1 are the zeroth and first-order Bessel functions, respectively. The form factor of the N* phase is modeled by oriented cylinders as[29]

$$P(q_\perp, q_z) = \left[\frac{2J_1(q_\perp R)}{q_\perp R}\frac{\sin(q_z L/2)}{q_z L/2}\right]^2$$

where q_z and $q_\perp$ are the wave vectors along and perpenticular to the rods, respectively. $P(q_\perp, q_z) \times S(q_\perp)$ is calculated for one nematic domain and then spherically averaged. The final model accounts for a Gaussian distribution of R and the instrumental resolution.

The fit shown in Figure 4 results in the following values: $\eta = 0.35$, the average hydrocarbon core radius of the cylinders $\bar{R} = 22.5$ Å, thickness of the hydrophilic shell = 5 Å, length of the cylinders = 4300 Å, core scattering length density (sld) = -4.3×10^{-7} Å^{-2}, shell sld = 3.2×10^{-6} Å^{-2}, and solvent sld = 6.38×10^{-6} Å^{-2}. Despite the approximations involved, the agreement between the calculated and observed $I(q)$ is very reasonable (Figure 4). More importantly, this model correctly predicts the q^{-1} decay seen at low q and confirms the presence of very long aggregates making up the N* phase, such as WLM. The length of the cylinder obtained from the model is at least 1 order of magnitude larger than the typical persistence length l_p of WLM in surfactant systems.[18] This is not surprising when we take into account the exponential dependence of l_p on the bilayer rigidity, κ,[30] and the fact that κ for phospholipids such as DMPC is almost an order of magnitude larger than that of typical surfactant bilayers.[31] However, one should bear in mind that the applied model is a first-order approximation, since the WLM are likely to have a noncircular cross-section, due to the preference of DMPC to form bilayers. Nevertheless, the agreement of the model with the data supports our conclusions on the morphology of the N* phase.

The behavior of the $Q = 2$ sample is very different in this intermediate temperature range. Although the viscosity increases at ∼25 °C, as in the other two samples, the N* phase appears only at 41 °C. It coexists with an isotropic phase, probably made up of bicelles, over its entire temperature range of stability. Both the N* and the viscous isotropic phases seem to be made up of entangled WLM. However, unlike in the $Q = 5$ and 3.2 samples, the bicelle to WLM morphology change of the aggregates is not reflected in the SANS data of this sample. This might be a consequence of either the presence of much shorter aggregates in the N* phase of $Q = 2$ samples or the much higher scattering from the coexisting isotropic micellar solution.

The turbidity seen in all of the samples at high temperatures is consistent with the presence of MLV. The MLV lamellar periodicity from all MLV samples is very close to that of pure DMPC MLV.[23,24] The q^{-4} dependence of the scattered intensity at low q is a reflection of Porod's law and indicates that the size of these large MLV is of the order of a few hundred nanometers.[32] The size of these MLV explains the very high turbidity of these samples and is consistent with the fact that at least some MLV can be seen under the optical microscope (Figure 3). The scattering pattern from this phase of a very dilute sample is characteristic of MLV dispersions (Figure 4). Concentrated samples show higher scattered intensity in the intermediate q range, which is reminiscent of the scattering profiles of some surfactant systems with low bilayer bending rigidity κ.[33] However, in phospholipids such as DMPC κ is generally almost an order of magnitude larger and, therefore, we do not know presently if the higher intensity in the intermediate q range is due to the structure factor of the solution or to the presence of other types of aggregates in the coexisting isotropic phase.

All of our observations can be rationalized, if we assume that the aggregate size R is determined by its DHPC content Q_a, R being larger for higher values of Q_a. As mentioned earlier, the low-temperature bicelle structure suggests segregation of DMPC and DHPC, with the former occupying the disk of the bicelle and the latter forming the rim. The observed phase behavior is consistent with a gradual decrease in the DHPC content of the mixed

(25) Danino, D.; Talmon, Y.; Levy, H.; Beinert, G.; Zana, R. *Science* **1995**, *269*, 1420.
(26) Ao, X.; Wen, X.; Mayer, R. *Physica A* **1991**, *176*, 63.
(27) Pelletier, O.; Bourgaux, C.; Diat, O.; Davidson, P.; Livage, J. *Eur. Phys. J. E* **2000**, *2*, 191.
(28) Rosenfeld, Y. *Phys. Rev. A* **1990**, *42*, 5978.
(29) Fournet, G. *Bull. Soc. Fr. Mineral. Cristallogr.* **1951**, *74*, 39.
(30) Chaikin, P. M.; Lubensky, T. C. *Principles of Condensed Matter Physics*; Cambridge University Press: Cambridge, 1995.
(31) Evans, E.; Rawicz, W. *Phys. Rev. Lett.* **1990**, *64*, 2094.
(32) *Small Angle X-ray Scattering*; Glatter, O., Kratky, O., Eds.; Academic Press: London, 1982.
(33) Yang, B.-S.; Lal, J.; Richetti, P.; Marques, C. M.; Russel, W. B.; Prud'homme, R. K. *Langmuir* **2001**, *17*, 5834.

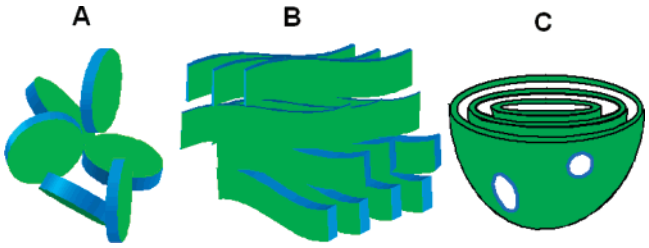

Figure 6. Schematic of the proposed aggregate morphologies in the system: bicelles (A), ribbons (B), and bilayers (C). The bicelle and ribbon edges are preferentially occupied by DHPC molecules, which also line the porelike defects dispersed in the bilayer. The bicelles form an isotropic phase, whereas in the N* phase the ribbons are orientationally ordered. The chirality of the system generates a spontaneous twist, with the twist axis normal to the long axes of the ribbons. The pitch of this helical structure is of the order of several micrometers. The bilayers are organized into MLV dispersed in an isotropic solution. Since these bilayers still have some amount of DHPC, it is possible that they contain some pores.

aggregates with increasing temperature, resulting in larger aggregates at higher temperatures. The proposed bicelle → ribbon → bilayer evolution of the aggregate morphology with temperature is in agreement with this picture (Figure 6). In the low-temperature isotropic phase, Q_a has the highest possible value in all three samples. On raising the temperature, there seems to be a sudden drop in Q_a at the DMPC chain melting transition, and larger ribbonlike aggregates start to form. In the $Q = 2$ sample, bicelles are also present at these temperatures and the sample continues to be isotropic. On the other hand, in the $Q = 3.2$ and 5 samples, the aggregates appear to be almost exclusively ribbons, which orientationally order to form a nematic phase. Due to the chirality of the lipid molecules, this phase develops a spontaneous twist, with the twist axis normal to the long axes of the ribbons. The noncircular cross-section of the ribbons probably results in a structure that is locally biaxial. There are two possible orientations of the twist axis, either along the major axis of the ribbon cross section or along its minor axis. Further experiments are necessary to determine which of these is selected in the present system. Increasing the temperature leads to further growth of the ribbons, and the viscosity of all the samples increases, as a result of increased ribbon entanglement. Interestingly, beyond some temperature the viscosity of these samples begins to decrease. In the $Q = 3.2$ sample, the viscosity maximum occurs at ~30 °C, which is well within the temperature range of the nematic phase (~23−53 °C) as determined from our microscopy studies.[20,21] This decrease in viscosity is most likely reflected by changes in the aggregate morphology. In this context, we note that a similar decrease in the viscosity of surfactant solutions containing WLM has been reported in the literature and is attributed to the formation of interconnections between the WLM.[34] The lower viscosity arises from the fact that these interconnections are not pinned to the WLM and can slide along it in order to relax the applied stress. A similar mechanism might be operating in the present system. Although the proximity of the lamellar phase lends further support to this conjecture, further work is required to confirm it.

4. Conclusion

We have characterized the phase behavior of DMPC−DHPC mixtures, which have been widely used as biomimetic membrane substrates for NMR studies of membrane-associated proteins and also for solution NMR studies of water-soluble macromolecules. All of the samples studied show an isotropic phase made up of disklike micelles, or so-called bicelles, below the T_M of DMPC. At higher temperatures, a chiral nematic phase is found, which transforms into a dispersion of MLV on further increasing T. The commonly used magnetically alignable nematic phase is found to consist of long, flexible wormlike micelles, and not bicelles as had been believed earlier. The high viscosity of this phase is a result of the entanglement of these polymer-like aggregates.

Abbreviations

DMPC	dimyristoyl phosphatidylcholine
DHPC	dihexanoyl phosphatidylcholine
DMPG	dimyristoyl phosphatidylglycerol
MLV	multilamellar vesicles
NMR	nuclear magnetic resonance
SANS	small-angle neutron scattering
POM	polarized optical microscopy
WLM	wormlike micelles

Acknowledgment. J.K. and M.-P.N. thank the Advanced Food and Materials Network (Guelph, Ontario) and the Neutron Program for Materials Research for financial support. This work utilized facilities supported in part by the National Science Foundation under Agreement No. DMR-9986442.

LA048641L

(34) Khatory, A.; Kern, F.; Lequeux, F.; Appell, J.; Porte, G.; Morie, N.; Ott, A.; Urbach, W. *Langmuir* **1993**, *9*, 933.